Modelling and
Simulation in Materials
Science and
Engineering

PAPER

Topology of SiO_x-units and glassy network of magnesium silicate glass under densification: correlation between radial distribution function and bond angle distribution

To cite this article: Nguyen Hung Son *et al* 2020 *Modelling Simul. Mater. Sci. Eng.* **28** 065007

IOP Publishing Modelling and Simulation in Materials Science and Engineering
Modelling Simul. Mater. Sci. Eng. **28** (2020) 065007 (30pp) https://doi.org/10.1088/1361-651X/ab9bb4

Topology of SiO_x-units and glassy network of magnesium silicate glass under densification: correlation between radial distribution function and bond angle distribution

Nguyen Hung Son[1], Nguyen Hoang Anh[1], Pham Huu Kien[2,4], Toshiaki Iitaka[3] and Nguyen Van Hong[1,4]

[1] Hanoi University of Science and Technology, Hanoi, Vietnam
[2] Institute of Research and Development, Duy Tan University, Da Nang, 550000, Vietnam
[3] Computational Engineering Applications Unit, Head Office for Information Systems and Cybersecurity, Riken, Japan

E-mail: phamhuukien@duytan.edu.vn and hong.nguyenvan@hust.edu.vn

Received 17 December 2019, revised 28 May 2020
Accepted for publication 11 June 2020
Published 15 July 2020

Abstract

Topology of SiO_x units and glassy network of magnesium silicate glass at different pressures are investigated by molecular dynamics simulation to clarify its microstructure under compression. Results show that SiO_x-topology and glassy network structure are significantly dependent on pressure. At ambient pressure, the –Si–O– glassy network in Mg_2SiO_4 glass is split into subnets/clusters. Under compression, the small subnets tend to merge each other forming larger ones. The decrease of Si–O–Si bond angle under compression that accompanies a formation of edge- and face-sharing bonds between SiO_x units results in the first peak splitting of Si–Si PRDF at high pressure. In particular, the investigation also reveals a tight correlation between PRDFs (Si–Si, Mg–Mg, Si–Mg, O–O) and BADs (Si–O–Si, Mg–O–Mg, Mg–O–Si, O–T–O (T = Si, Mg)), respectively. The spatial distribution of corner-, edge- and face-sharing bonds is not uniform but forming subnets/clusters. The clusters of face-sharing bonds form rigid particles embedding into mixture clusters of corner- and edge-sharing bonds. Size distribution of subnets/clusters (SiO_x-cluster as well as clusters of corner-, edge- and face-sharing bonds) under compression also has been investigated to clarify the intermediate range order.

[4]Authors to whom any correspondence should be addressed.

0965-0393/20/065007+30$33.00

The characteristic change of PRDFs under compression in the relationship with microstructural change and the mechanism of magnesium ions incorporation into –Si–O– network is also discussed in detail.

Keywords: correlation, microstructure, compression, simulation, molecular dynamics

(Some figures may appear in colour only in the online journal)

1. Introduction

Silica and magnesium-silicate (SiO_2, $MgSiO_3$, Mg_2SiO_4) are important constituents of both commercial display glass and the Earth's mantle. Understanding the short- and intermediate-range order (SRO and IRO) as well as –Si–O– glassy network structure is very important for many scientific and technological fields (material science and geosciences). Therefore, the microstructure of magnesium silicate has been investigated for many decades [1–16]. For $MgSiO_3$ and Mg_2SiO_4 glasses, neutron scattering and x-ray diffraction experiments [8, 9] showed that: Si atoms have tetrahedral coordination forming SiO_4 tetrahedra with the average Si–O distance of approximately 1.60–1.64 Å; Mg atoms have mean coordination number of 4.5 $\pm$ 0.1 (an approximately equal mixture of MgO_4 and MgO_5 polyhedra) and 5.0 $\pm$ 0.1 corresponding to $MgSiO_3$ and Mg_2SiO_4 glasses. The Mg–O distance is of approximately 2.00 Å. The Mg–O peak in the plot of neutron total structure factors is asymmetric and has high-r tail. This reveals a distorted magnesium coordination polyhedron and a broad distribution of Mg–O bond distances.

NMR experiments [10, 11] reveal that Mg–O coordination consists of both five-fold and six-fold in that six-fold is dominant in both $MgSiO_3$ and Mg_2SiO_4 systems. In contrast, by coupling x-ray and neutron diffraction with a reverse Monte Carlo (RMC) simulation, authors in work [14] have shown that Mg in $MgSiO_3$ has average coordination number of 4.5, similar to the reported result in [8]. Besides, a similar study reported that the average coordination number of Mg is around 5.1 (mixture of MgO_4, MgO_5 and MgO_6 polyhedra) [15]. Based on the results of the x-ray and neutron diffraction experiments, it reveals that the structure of $MgSiO_3$ glass comprises MgO_4 and MgO_5 polyhedra, which are connected to the silicate network by corner-sharing bonds with SiO_4 tetrahedra. Experimental data and RMC simulation in [6, 16] have shown that the population of MgO_4, MgO_5, and MgO_6 polyhedra is about 68.8%, 27.8%, and 3.4%, respectively. Considering the local structure of Mg ions, investigation results revealed that Mg–O bond distances in MgO_4 coordination units are shorter than the one in other coordination units (MgO_5 and MgO_6). For $MgSiO_3$ system, the average Mg–O bond in MgO_4 and MgO_6 coordination units is about 1.924 Å and 2.10 Å respectively [11–18]. For the SiO_4 tetrahedral network, investigation results show that the tetrahedral network structure in $MgSiO_3$ comprises Q^1, Q^2 and Q^3 units in that Q^3 is dominant (here Q^n is the SiO_4 units with n bridging oxygens (BO); the O atoms that connect to at least two Si atoms are considered as BO). The oxygens that only bind to Mg are considered as free oxygens (FO) [7, 17].

Besides experimental methods, simulation is also a useful method to investigate microstructure of glasses and melts, especially at high temperature and pressure. The results of molecular dynamics simulation in [19] showed that the average Mg–O distance in MgO_4 polyhedra is about 1.92–1.98 Å. However, report in [20] showed that four O^{2-} ions are bonded to each Mg^{2+} ion at Mg–O distance about 2.00 Å and two more O^{2-} ions at distance 2.20 Å.

This is in good agreement with a recent MD simulation that revealed six-fold coordinated Mg. Mg ions with octahedral-coordination forms distorted MgO_6 octahedra with the average Mg–O distance of 2.07 Å and average coordination number of 5.7. Simulation of magnesium-silicate melts under compression shows that coordination number of Si increases from four-fold at low pressure to six-fold at higher pressure. It means that there is a structural change under densification [21–23]. Results also show that the number of free oxygen and oxygen with one or two nearest Si and/or Mg neighbors decreases whereas the number of O with three or over three nearest Si and/or Mg neighbors increases with pressure [21, 24]. By MD simulation [25], the authors show that in the 0–24 GPa pressure range, the structure of magnesium silicate melts is taken up mostly by the change of IRO. This is shown by the variation of the Si–O–Si bond angle. By using *ab initio* molecular dynamics simulation for $MgSiO_3$ melt at ultrahigh pressure and temperature [26], the authors have shown that in 230.1–464.7 GPa pressure range and at temperature of 13 000 K, the average Si–O coordination number increases nearly linearly from 6.4 to 7.3 while the Mg–O and O–O coordination numbers are about 8.1–8.3 and 9.6–9.9, respectively (almost unchanged with pressure). This result indicates no sign of a first-order liquid–liquid phase transition. In the work [27], by mean of first-principles MD simulations for $MgSiO_3$ glass at 300 K in the 0–170 GPa pressure range, the authors have shown that: at ambient pressure the first peak position of Si–O, Mg–O, O–O, Si–Si, Mg–Si and Mg–Mg pairs are 1.63, 1.98, 2.68, 3.00, 3.19 and 2.92, respectively. This result is in good agreement to the results reported in works [11–17, 28–35, 39, 40]; the corresponding mean coordination numbers of the Si–O, Mg–O, O–O, Si–Si, Mg–Si and Mg–Mg pairs are 4.0, 4.6, 5.8, 2.1, 4.6 and 4.5. Under compression, mean coordination numbers of Si–O and Mg–O increase from 4.0 and 4.6 (at ambient pressure) to 6.0 and 8.0 (at 170 GPa), respectively. The average Mg–O bond length is about 2.08 Å and almost not dependent on pressure in 0–15 GPa range. At pressure beyond 15 GPa, the average Mg–O bond length decrease linearly with pressure and get the value of approximately 1.94–1.96 Å at 170 GPa. The average Si–O bond length increases with pressure in the 0–40 GPa range. The average Si–O bond at 40 GPa is about 1.74 Å. At pressure beyond 40 GPa, the average Si–O bond length decreases linearly with pressure and get the value of around 1.66–1.67 Å. Results also showed that under compression the PRDFs of Si–O, Mg–O, O–O, Si–Si, Mg–Si and Mg–Mg pairs are strongly dependent on pressure. In particular, the first peak of Si–Si, Mg–Si pair PRDFs splits into two sub-peaks at high pressure. However, the cause of the change of PRDFs as well as the first peak splitting of Si–Si, Mg–Si pair PRDFs is not explained clearly [43].

Studies of magnesium silicate by molecular dynamics simulation have been reported in many works [19–40]. Most of them focus on investigation of the structural and dynamical characteristics (at different compositions, densities and temperatures) such as: diffusion and viscosity [19, 20, 28, 29]; structural transformation [40]; distribution of bond distance, bond angle, coordination number, and Q^n species [19–21, 23–26, 39]. The reference [39] is the typical work that investigated the structure of magnesium silicate at different composition ($_xMgO_{100-x}SiO_2$ *with x= 50, 54, 58, 62 and 67; the models with the size from 1000–1230 atoms*) and pressure (*at 0, 8.6 and 9.0 GPa*). The structural characteristics such as partial correlation functions, coordination numbers, bond angle distribution and connectivity have been investigated and compared to diffraction experiment and crystal models.

In the present work, a large-scale molecular dynamics simulation is performed for a Mg_2SiO_4 system consisting of 4998 atoms. The structural characteristics such as radial distribution function, coordination number, bond angle distribution, bond length distribution, size distribution of clusters/subnets and distribution of OT_y linkages (T = Si, Mg; y = 2–7)

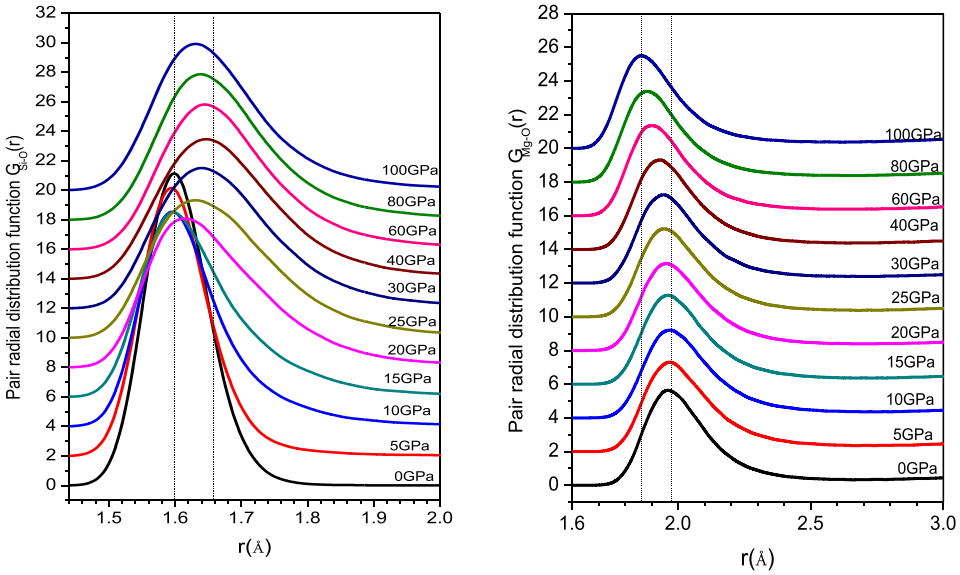

Figure 1. Pair radial distribution function for Si–O and Mg–O pair at different pressures (the vertical line is added into the plot to show the change of peak position under compression).

have been investigated in detail to clarify the following issues: local structure and topology of SiO_x units; intermediate range order and correlation between PRDFs and corresponding BADs; glassy network structure; mechanism of Mg ion incorporation into –Si–O– glassy network.

2. Calculation method

The models of Mg_2SiO_4 glass consisting 4998 atoms (714 Si atoms, 2856 O atoms, and 1428 Mg atoms) are constructed by MD simulation at 600 K and in the 0–100 GPa pressure range with boundary conditions for all three dimensions. The Oganov potentials which have been successfully used for structural and dynamical simulation of magnesium silicate systems (both in glass and melt states) were applied in this work. The detail about the Oganov potential can refer to works [21, 29–35] .

MD program is written by C language using Verlet algorithm with MD time step of 0.47 fs (the program is written by ourselves). The initial configuration of model is generated by placing all atoms randomly in a simulation cell with density of 3.22 g cm^{-3} (real density of crystal Mg_2SiO_4) [41, 42]. Next the model is heated up to 6000 K to assure that the initial configuration of model is removed [35]. At temperature of 6000 K, the model is relaxed for 10^5 MD time steps. After that the model is cooled down to 5000, 4000 (at each temperature the model is also relaxed for 10^5 MD time steps), and finally to 3500 K. Next, the model is relaxed for a long time (10^6 MD time step) in ensemble NPT (constant temperature and pressure) to produce a model at 3500 K and upon ambient pressure, called M0. Next, different models at temperature of 3500 K and pressures of 0, 5, 10, 15, 20, 25, 30, 40, 60, 80 and 100 GPa are produced by compressing model M0 to corresponding pressures. Next, the models are cooled to 600 K with cooling rate of 2.5 K ps^{-1}. After that, the models at

Table 1. Comparison of the structural characteristics to experimental data and simulation from *ab initio*

	This work, MD ($P = 0$, $T = 600$ K) (Å)	De koker *et al* [24] *ab initio* ($T = 3000$ K) (Å)	Kohara *et al* [38], experiment ($P = 0$ GPa; $T = 300$ K glass) (Å)
$d_{\mathrm{Mg-O}}$	1.98	1.97	2.00
$d_{\mathrm{Si-O}}$	1.60	1.63	1.63
$Z_{\mathrm{Mg-O}}$	4.75	5.10	5.00
$Z_{\mathrm{Si-O}}$	4.00	4.10	4.10

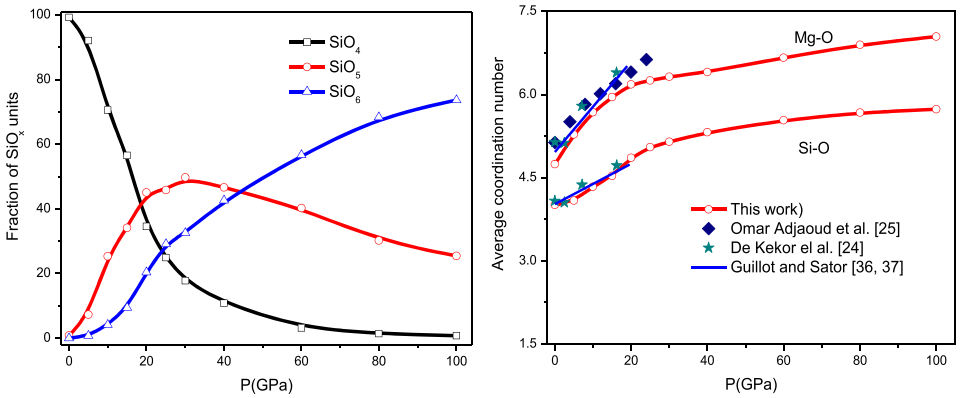

Figure 2. Si–O and Mg–O coordination number as a function of pressure. For comparison, we have included simulation results from *ab initio* (De Koker *et al*, [24]) at 3000 K and rigid ion simulations (Guillot and Sator, [36, 37]) on peridotite liquid at 2273 K and MD simulation with flexible potential model (Omar Adjaoud *et al* [25]) on Mg_2SiO_4 melt at temperature between 2390 K and 3200 K.

600 K and different pressures (0, 5, 10, 15, 20, 25, 30, 40, 60, 80 and 100 GPa) are relaxed for 10^6 MD time steps.

The structural characteristics of each model are determined by averaging over 1000 configurations during the last 5×10^4 MD steps. To calculate the clusters as well as coordination number, the cutoff distance is chosen based on the minimum position after the first peak of the PRDF. Namely, for Si–O pair, the cutoff distance is 2.2 Å.

3. Results

3.1. Local structure and topology of SiO_x units

Figure 1 shows the PRDFs of Si–O and Mg–O pairs at different pressures. It can be seen that in the 0–15 GPa pressure range, the first peak position of Si–O PRDF is at around 1.60 Å and almost not dependent on pressure. At pressure beyond 15 GPa, the first peak position of Si–O PRDF tends to shift to right with the increase of pressure (up to 40 GPa). Its location at 40 GPa is 1.66 Å. At pressure beyond 40 GPa, the first peak position of Si–O PRDF tends to shift to left. Its location at 100 GPa is around 1.62–1.64 Å. In contrast, in the 0–100 GPa pressure range, the first peak position of Mg–O PRDF tend to shift to the left as pressure

increases, from location of 1.98 Å (at ambient pressure) to 1.85 Å (at 100 GPa). Table 1 show the comparison of the structural characteristics of Mg_2SiO_4 model in this study (at ambient pressure) to experimental data and simulation from *ab initio*. It can be seen that the average Mg–O and Si–O bond lengths and coordination numbers at ambient pressure rather agree with both experimental data [38] and simulation from *ab initio* [24]. Figure 2 shows the Si–O and Mg–O coordination number distribution as a function of pressure. It can be seen that at ambient pressure, all Si ions have coordination of 4.0 forming SiO_4 units. It means that the average Si–O coordination number is 4.0 at ambient pressure. As pressure increases, the number of four-fold coordinated Si ions decreases, meanwhile the number of five- and six-fold Si ions increases forming SiO_5 and SiO_6 units [8–15, 19–25]. The concentration of SiO_5 increases with pressure and get maximum value (approximately 50%) at around 30 GPa. At pressure beyond 30 GPa, the concentration of SiO_5 decreases with pressure. At pressure of 100 GPa, the concentration of SiO_5 is 25.3%. The number of six-fold Si ions increases monotonically with pressure and get the value of 73.5% at pressure of 100 GPa. The average Si–O coordination number increase strongly with pressure up to 30 GPa. The average Si–O coordination number at 30 GPa is approximately 5.20. At pressure beyond 30 GPa, the average Si–O coordination number increases slightly with pressure. It gets value of 5.73 at 100 GPa [23–35]. The average Mg–O coordination number increases strongly from 4.75 at ambient pressure to 6.18 at 20 GPa. At pressure beyond 20 GPa, the average Mg–O coordination number increases slightly with pressure and get the value of 7.04 at 100 GPa. The change of average Mg–O and Si–O coordination numbers under compression rather agrees with simulation from *ab initio* [24] as well as rigid ion simulations [36, 37] on peridotite liquid at 2273 K and MD simulation with flexible potential model [25].

Figure 3 shows the O–Si–O bond angle and Si–O bond length distribution (BAD and BLD) in SiO_x at different pressures. It can be seen that the O–Si–O bond angle in SiO_4 has the Gaussian form and changes slightly with pressure. As pressure increases, the O–Si–O BAD in SiO_4 units tend to shift slightly to left and a little broader. This makes the height of the peak decrease significantly with the increase of pressure. In contrast, the O–Si–O BAD in SiO_5 units have a main peak at approximately 90° and a shoulder at around 170°, and it almost does not change with pressure. The O–Si–O BAD in SiO_6 units has a main peak at around 85° and a small peak at 170°. As pressure increases, the BAD is a little broader and the height of the peak change significantly [26, 34, 35, 39].

For Si–O BLD in SiO_x, from figure 3, it can be seen that the Si–O BLDs in SiO_4, SiO_5 and SiO_6 have the Gaussian form and they tend to shift slightly to left as pressure increases. At ambient pressure, the Si–O BLD in SiO_4 has the peak at location of around 1.60 Å [8, 9, 11, 35–37]. At pressure of 40 GPa, the peak shifts to the location of approximately 1.56–1.58 Å. At low pressure (5 GPa), the Si–O BLD in SiO_5 has the peak at location of around 1.68 Å. In the 0–30 GPa pressure range, it shifts slightly to left with the increase of pressure. At pressure beyond 30 GPa, it shifts significantly to the left with the increase of pressure. At 100 GPa, the peak position is at around 1.60 Å. Similar to the Si–O BLD in SiO_5 units, the Si–O BLD in SiO_6 at low pressure (10 GPa) has the peak at around 1.72 Å. In the 0–30 GPa pressure range, it changes slightly with pressure. At 30 GPa, the peak of Si–O BLD in SiO_6 locates at around 1.70 Å. At pressure beyond 30 GPa, it decreases significantly with pressure and its position at 100 GPa is around 1.64 Å. The above analysis reveals that the Si–O bond length in SiO_6 is longer the one in SiO_5 and the one in SiO_5 is longer than the one in SiO_4.

From figure 1, it also reveals that the average Si–O bond length at low pressure is about 1.60 Å and it tends to increase with pressure and gets maximum value of approximately 1.66 Å at 40 GPa. At pressure over 40 GPa, the average Si–O bond length tends decrease

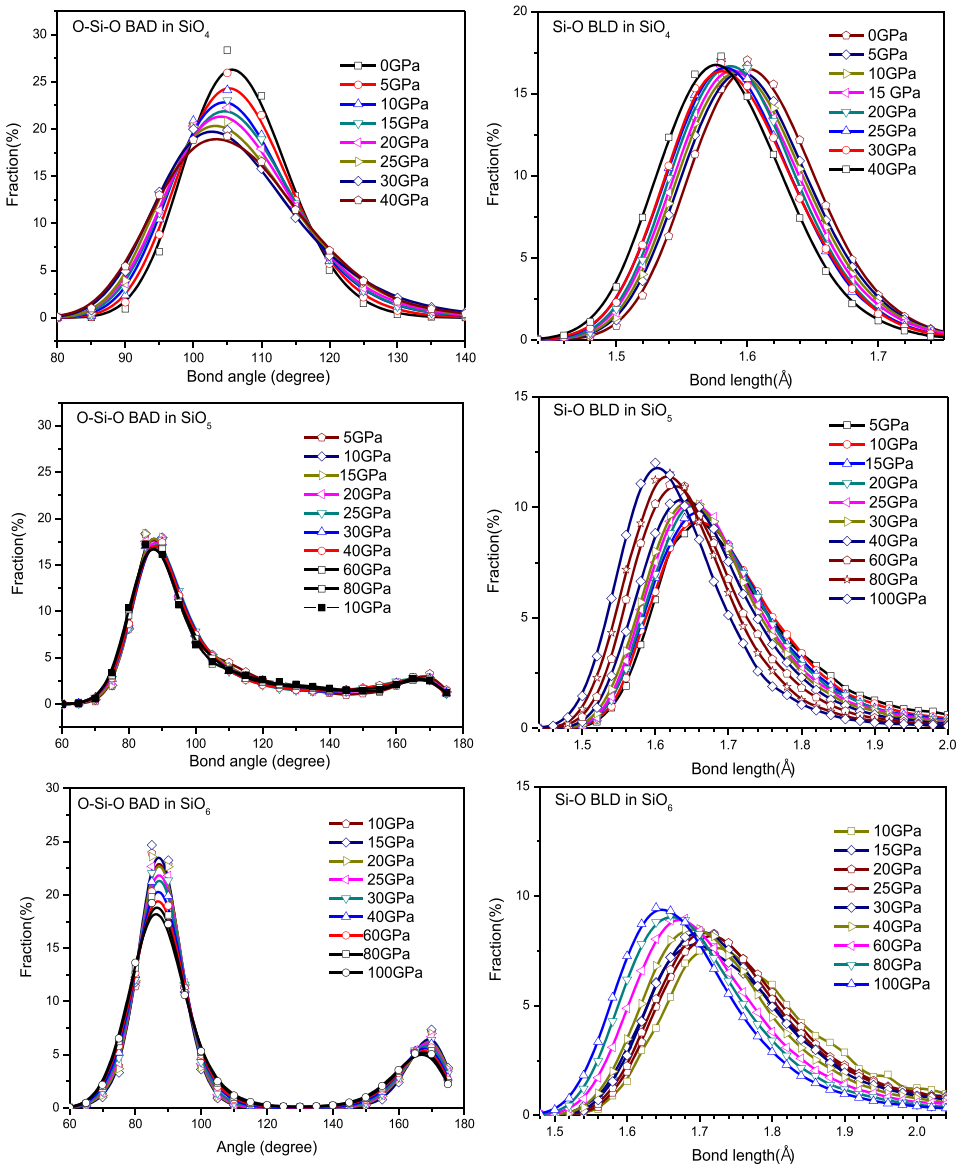

Figure 3. Bond angle and bond length distribution in SiO_x ($x = 4, 5, 6$) at different pressures.

with pressure. At 100 GPa, the average Si–O bound length has the value of approximately 1.62–1.64 Å. The change of average Si–O bond length is based on the competition of the increase due to the increases average Si–O coordination number and the decrease due to the compression. In the 0–40 GPa range, the increase of Si–O bond length due to the increases of coordination is very large in comparison to its decrease due to the compression, so average Si–O bond length increases with pressure. At pressure beyond 40 GPa, the increase of average Si–O bond length due to the increases of coordination is smaller than its decrease due to the compression, so Si–O bond length decreases with pressure.

The Si–O bond length in SiO_4 < the ones in SiO_5 < the ones in SiO_6. The difference of Si–O bond length among SiO_4, SiO_5 and SiO_6 can be explained as following: the average O–Si–O bond angle in SiO_4 is larger than the one in SiO_5 and SiO_6, see figure 3. Therefore, the average O–O distance in SiO_5 and SiO_6 units is smaller than the one in SiO_4. This leads to increasing the Coulomb repulsion between O^{2-} and O^{2-} ions and this leads to elongation of the Si–O bond length. So that, the Si–O bond length in SiO_4 units is smaller the one in SiO_5 and SiO_6. In other word, the increase of Si–O coordination number leads to the increase of Si–O bond length, similar to the increase of Si–O bond length in pure SiO_2 glass under compression [41].

For Mg–O bond length, the Mg–O PRDF reveals that the average Mg–O bond length tends to decrease with pressure. At ambient pressure, the average Mg–O bond length is 1.98 Å. This value decreases to 1.85 Å at 100 GPa. It means that the increase of Mg–O coordination number does not result in the increase of average Mg–O bond length. This can be explained as following: The MgO_n (with $n = 4$–10) is not stable; the Mg–O bond length distributes in a wide range; the Mg–O bond length is longer than the Si–O. Therefore, the increase of Mg–O bond length due to the increase of Mg–O coordination number is rather small in comparison to its decrease due to compression. In other words, with increasing pressure, the increase of Mg–O bond length due to the increase of Coulomb repulsion between O^{2-} and O^{2-} ions is very small in comparison with its decrease due to compression. That is why the average Mg–O bond length decreases with the increase pressure.

The increase of SiO_5 and SiO_6 concentration under compression results in the increase of the average Si–O bond length. In the 0–40 GPa, the concentration of SiO_5 and SiO_6 increases strongly with pressure leading to the increase of average Si–O bond length. That is why the first peak of Si–O PRDF shifts to right, see figure 1. At pressure beyond 40 GPa, the increase of SiO_6 concentration is accompanied by the decrease of SiO_5 concentration. It means that the total concentration of SiO_5 and SiO_6 unit is almost not change. In addition, at pressure beyond 40 GPa, the Si–O bond length in SiO_5 and SiO_6 decreases strongly with pressure. Therefore, in the 40–100 GPa pressure range, the average Si–O bond length decreases with the increase of pressure, see figure 1. This explains why the first peak of Si–O PRDF shifts to left as pressure increase in the 40–100 GPa range, as showed in figure 1. The above results also reveal that the topology structure of SiO_5 and SiO_6 units is stable at high pressure. The form of SiO_5 and SiO_6 units almost does not change with pressure. However, their size is decreases with the increases of pressure. In contrast, the SiO_4 units are not stable at high pressure. The SiO_4 tetrahedra is more distorted under compression.

3.2. Intermediate range order and correlation between PRDFs and corresponding BADs

The intermediate range order relates to the interconnect among SiO_x and MgO_n. Their characteristics are shown in the Si–Si, Mg–Mg, Mg–Si and O–O PRDFs. Figure 4 shows the Si–Si PRDF and Si–O–Si BAD at different pressures. It can be seen that at low pressure ($P \leqslant 15$ GPa), the Si–Si PRDF has the first peak at location of approximately 3.00–3.10 Å. At pressure beyond 15 GPa, it appears a shoulder at around 2.80 Å beside the first main peak at location of 3.00–3.10 Å. At pressure beyond 30 GPa, the shoulder becomes a sub-peak. The height of the sub-peak increases with pressure and it tends to shift slightly to the left with the increase of pressure. At pressure beyond 60 GPa, the first peak of Si–Si PRDF splits into two peaks, the main one at location of approximately 3.08–3.10 Å and the small one at around 2.60 Å. The first peak splitting of Si–Si PRDF can be explained as following: the Si–Si distance can be determined from Si–O–Si bond angle and the Si–O bond length. Namely, the Si–Si distance

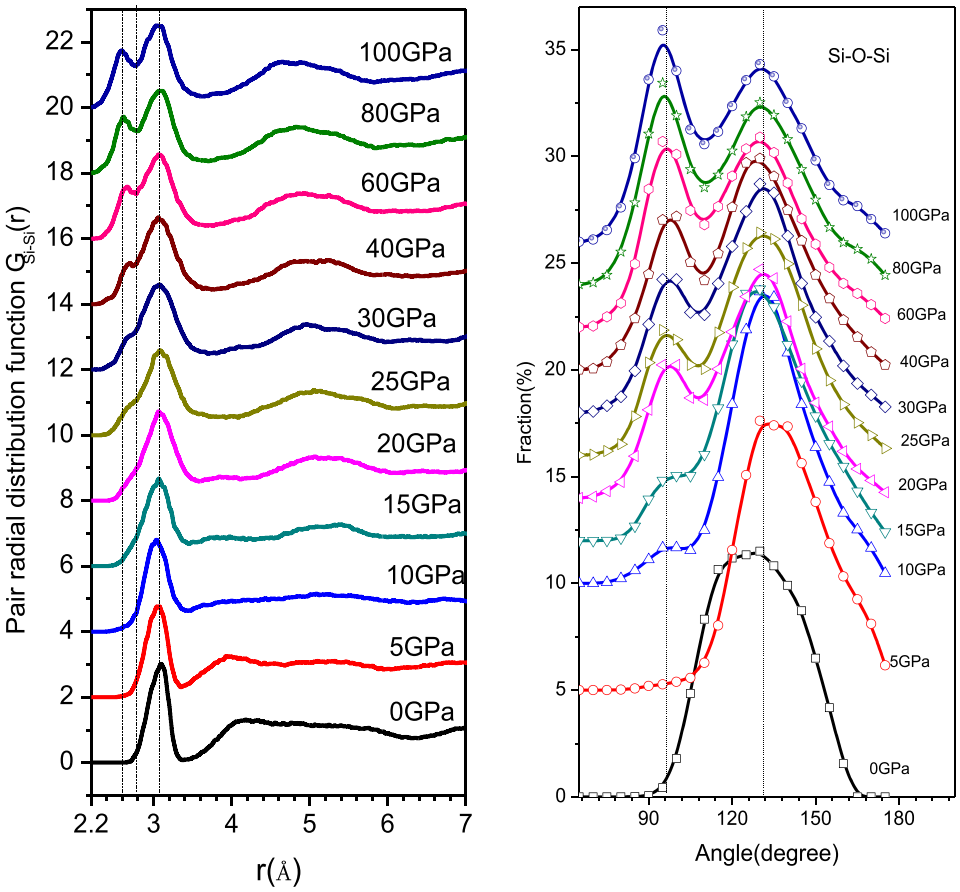

Figure 4. The Si–Si PRDF and Si–O–Si bond angle distribution at different pressures (the vertical line is added into the plot to show the change of peak position under compression).

can be calculated by equation (1).

$$d_{\mathrm{Si-Si}} = \sqrt{d_{\mathrm{Si-O}}^2 + d_{\mathrm{Si-O}}^2 - 2 * d_{\mathrm{Si-O}} * d_{\mathrm{Si-O}} * \cos\left(\mathrm{Si}\widehat{-\mathrm{O}-}\mathrm{Si}\right)}. \tag{1}$$

Here $d_{\mathrm{Si-Si}}$ is the Si–Si distance, $d_{\mathrm{Si-O}}$ is the Si–O bond length and the $\mathrm{Si}\widehat{-\mathrm{O}-}\mathrm{Si}$ is the Si–O–Si bond angle (call T–O–T angle as α from now, T = Si, Mg). At low pressure ($P \leqslant 15$ GPa), the Si–O–Si BAD has one peak at around 132–135° [25], the Si–O bond length is about 1.60–1.62 Å. With $d_{\mathrm{Si-O}} \sim 1.60$–1.62 Å and $\alpha \sim 132$–135°, then $d_{\mathrm{Si-Si}}$ is about 2.96–3.07 Å. The value of Si–Si distance that is calculated by equation (1) corresponding to the location of the main peak of Si–Si PRDF (around 3.00–3.10 Å), see figure 4. At pressure beyond 15 GPa, the Si–O–Si BAD has two peaks at around 95–98° and 132–135°. The Si–Si bond distance that is calculate by equation (1) with $d_{\mathrm{Si-O}} \sim 1.60$–1.66 Å and $\alpha \sim 95$–98° is around 2.40–2.60 Å. The one with $\alpha \sim 132$–135° is around 2.90–3.07 Å. These two values of Si–Si bond length correspond to the two first peaks of Si–Si PRDF, see figure 4. The above analysis reveals that the Si–Si distance can be determined by equation (1). The calculated results are in good

Table 2. The average number of corner-, edge- and face-sharing bonds per one Si atom at different pressures. N_c, N_e and N_f are the average number of corner-, edge-, and face-sharing bonds per one Si atom, respectively.

	Si–Si		
P (PGa)	N_c	N_e	N_f
0	0.68	0.00	0.00
5	0.75	0.01	0.00
10	0.90	0.04	0.00
15	0.98	0.07	0.00
20	1.16	0.11	0.01
25	1.23	0.18	0.01
30	1.29	0.21	0.02
40	1.37	0.25	0.03
60	1.38	0.38	0.03
80	1.42	0.40	0.03
100	1.47	0.42	0.04

agreement with simulated data. It also demonstrates that there is a tight correlation between Si–Si PRDF and Si–O–Si BAD. The first peak splitting of Si–Si PRDF under compression relates to the change of IRO. Namely, it is the change of the interconnection among SiO_x units in –Si–O–Si– glassy network. At low pressure, most of SiO_x units link to each other via one common O (corner-sharing bond). At high pressure, in –Si–O–Si– network form edge-sharing bonds (two SiO_x units link to each other via two common O) and face-sharing bonds (two SiO_x units link to each other via three common O). Table 2 shows the average number of corner-, edge- and face-sharing bonds per one Si atom at different pressures. It can be seen that the average number of edge- and face-sharing bonds per one Si atom increase with increasing pressure.

Table 3 shows the average bond length of corner-, edge- and face-sharing bonds between SiO_x–SiO_x at different pressures. It can be seen that in the considered pressure range, the average bond length of corner-sharing bonds is around 3.02–3.12 Å. This value corresponds to the location of the first main peak of Si–Si PRDF. The average bond length of edge-sharing bonds is around 2.80 Å. This value corresponds to the location of the shoulder beside the first main peak (at pressure beyond 20 GPa), see figure 4. The average bond length of face-sharing bonds is around 2.50–2.60 Å. This value is very near the location of the small peak (at pressure beyond 40 GPa). There are three bond types (corner-, edge- and face-sharing bonds) but the Si–Si PRDF only has two peaks. This is due to the fact that the average length of edge-sharing bonds is very near to the one of face-sharing bonds. Therefore, they merge each other into the one peak at location around 2.60 Å.

Figure 5 shows the Mg–Mg PRDF and Mg–O–Mg BAD at different pressures. It can be seen that, the first peak position of Mg–Mg PRDF shifts gradually to the left with increasing pressure. At ambient pressure, the first peak position is at around 2.80–3.00 Å. At high pressure (beyond 60 GPa), it is at around 2.60–2.80 Å. Besides, at pressure beyond 15 GPa, on the Mg–Mg PRDF, it appears a shoulder at location of 3.60–3.80 Å, on the right of the first peak. The height of the shoulder increases with pressure and it becomes the small peak at pressure beyond 40 GPa. The change of Mg–Mg PRDF under compression has the correlation to the change of the Mg–O–Mg BAD. It means that the change of the interconnection between MgO_x under compression is revealed on Mg–Mg PRDF. At ambient

Table 3. The average bond length of corner-, edge- and face-sharing bond between SiO_x-SiO_x at different pressure. Here, CSBL, ESBL and FSBL are the average bond length of corner-, edge- and face-sharing bonds, respectively.

P (GPa)	CSBL (Å)	ESBL (Å)	FSBL (Å)
0	3.08	—	—
5	3.08	2.79	—
10	3.09	2.78	2.54
15	3.09	2.79	2.60
20	3.12	2.80	2.61
25	3.11	2.80	2.50
30	3.10	2.85	2.49
40	3.09	2.84	2.52
60	3.06	2.87	2.51
80	3.04	2.83	2.52
100	3.02	2.79	2.54

pressure, the Mg–O–Mg BAD has a peak at location of around 85–90°. From the value of Mg–O–Mg bond angle ($\alpha \sim 85$–90°) and the Mg–O bond length (1.85–1.98 Å). The first peak location of Mg–Mg PRDF (the Mg–Mg distance) can be determined via equation (2). According equation (2), the Mg–Mg distance is about 2.80–2.85 at ambient pressure and about 2.62 Å at high pressure. These Mg–Mg distance calculated via equation (2) is in good agreement with simulation results, see the Mg–Mg PRDF in figure 5.

$$d_{\mathrm{Mg-Mg}} = \sqrt{d^2_{\mathrm{Mg-O}} + d^2_{\mathrm{Mg-O}} - 2 * d_{\mathrm{Mg-O}} * d_{\mathrm{Mg-O}} * \cos\left(\mathrm{Mg}\widehat{-\mathrm{O}-}\mathrm{Mg}\right)}. \quad (2)$$

At pressure beyond 15 GPa, the Mg–O–Mg BAD appear shoulder at location of around 145°. With Mg–O–Mg bond angle of 145°, the corresponding Mg–Mg distance that is calculated via equation (2) is about 3.70–3.80 Å. This value corresponds to the location of the shoulder on the Mg–Mg PRDF in figure 5.

Figure 6 shows the Si–Mg PRDF and Si–O–Mg BAD at different pressures. It can be seen that, at ambient pressure, the Si–Mg PRDF has a peak at location of approximately 3.20–3.40 Å. The peak shifts gradually to the left with increasing pressure. At pressure beyond 20 GPa, the peak is at location of approximately 2.80 Å. At pressure beyond 60 GPa, the peak is at location of around 2.60 Å. The characteristics of the Si–Mg PRDF has the correlation to the interconnection between SiO_x and MgO_n units. The change Si–Mg PRDF under compression relates to the change of the Si–O–Mg BAD.

$$d_{\mathrm{Si-Mg}} = \sqrt{d^2_{\mathrm{Si-O}} + d^2_{\mathrm{Mg-O}} - 2 * d_{\mathrm{Si-O}} * d_{\mathrm{Mg-O}} * \cos\left(\mathrm{Si}\widehat{-\mathrm{O}-}\mathrm{Mg}\right)}. \quad (3)$$

The first peak position of Si–Mg PRDF (Si–Mg distance) can be determined from equation (3). Figure 6 shows that at ambient pressure, the Si–O–Mg BAD has a peak at location of 120° and a shoulder at location of 90°. The height of the peak decreases with increasing pressure. While the height of shoulder increase with increasing pressure. At pres-

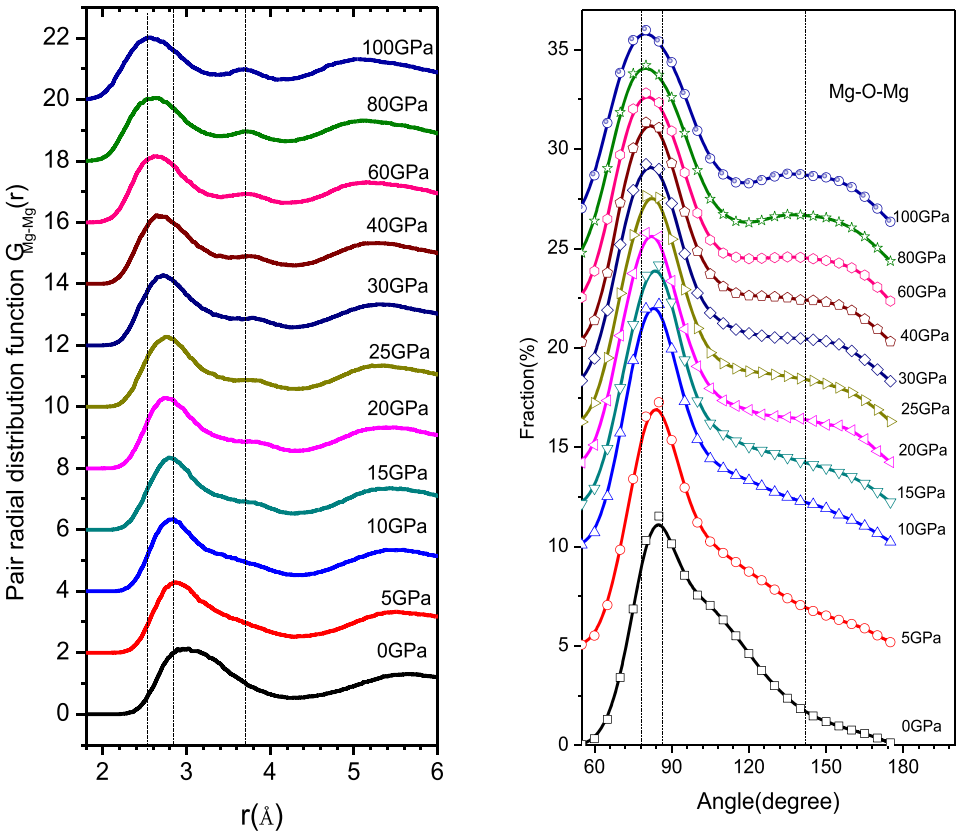

Figure 5. The Mg–Mg PRDF (left) and Mg–O–Mg bond angle distribution (right) at different pressures (the vertical line is added into the plot to show the change of peak position under compression).

sure beyond 10 GPa, the shoulder at location 90° becomes the peak, while the peak at location 120° becomes the shoulder. At ambient pressure, the Si–O–Mg bond angle is about 120°. The value of Si–Mg distance calculated by equation (3) is about 3.28–3.32 Å. At high pressure, with Si–O–Mg bond angle of around 93–95°, the Si–Mg distance is about 2.60–2.80 Å. These values are in good agreement with simulation results, see Si–Mg PRDF on figure 6 and tables 4 and 5. It reveals that there is a tight correlation between the characteristics of Si–Mg PRDF and corresponding Si–O–Mg BAD. It can be seen that the Si–Mg distance of 3.28–3.32 corresponds to corner-sharing bonds. The Si–Mg distance of about 2.60–2.80 Å corresponds to edge- and face-sharing bonds, see tables 4 and 5.

Figures 7 and 8 show the O–O PRDF, O–Si–O and O–Mg–O BADs at different pressures. At ambient pressure, the O–O PRDF has two peaks. The main peak at locations of around 2.60 Å and the small peak at around 2.90 Å. The small peak location shifts gradually to the left with increasing pressure. At pressure beyond 20 GPa, the two peaks merges into a single peak at location of around 2.60 Å.

The O–O PRDF has the correlation to the O–Si–O and O–Mg–O bond angle. At ambient pressure, the O–Si–O BAD has a peak at 105–110° and the O–Mg–O BAD has a peak at about 85–90°. The O–O distance in SiO_x calculated via equation (4a) is about 2.50–2.60 Å

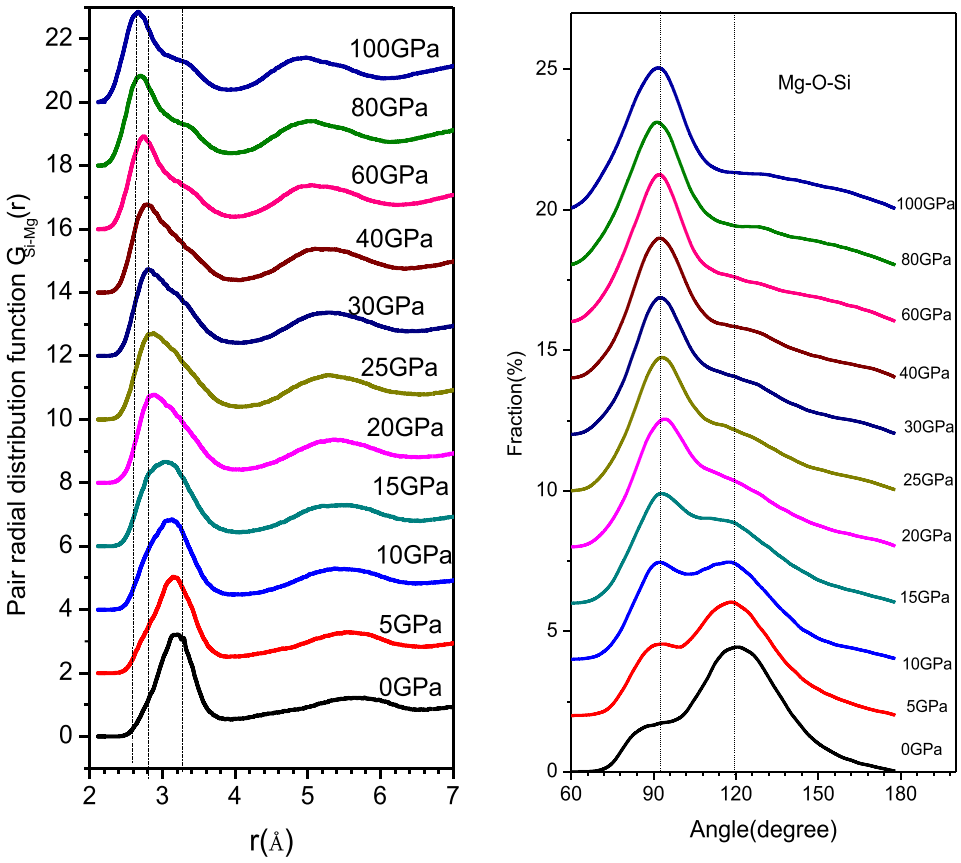

Figure 6. The Si–Mg PRDF (left) and Si–O–Mg bond angle distribution (right) at different pressures (the vertical line is added into the plot to show the change of peak position under compression).

corresponding the main peak in O–O PRDF. The O–O distance in MgO_n calculated via equation (4b) is about 2.80–2.90 Å corresponding the small peak in O–O PRDF.

$$d_{O-O}^{SiO_x} = \sqrt{d_{Si-O}^2 + d_{Si-O}^2 - 2 * d_{Si-O} * d_{Si-O} * \cos\left(O - \widehat{Si} - O\right)} \tag{4a}$$

$$d_{O-O}^{MgO_n} = \sqrt{d_{Mg-O}^2 + d_{Mg-O}^2 - 2 * d_{Mg-O} * d_{Mg-O} * \cos\left(O - \widehat{Mg} - O\right)}. \tag{4b}$$

The above analysis demonstrates that the main peak at 2.60 Å corresponds to the O–O distance in the SiO_x. The peak at 2.90 Å corresponds to the O–O distance in the MgO_n.

The peak position of O–Si–O and Mg–O–Mg BAD shift gradually to left with increasing pressure. At pressure beyond 40 GPa, the peak of the O–Si–O and Mg–O–Mg BADs is around 85–90° and 80–85° respectively. With these O–Si–O and Mg–O–Mg bond angle,

Table 4. The average number of corner-, edge- and face-sharing bonds per one atom (Si or Mg) at different pressures. N_c, N_e and N_f are the average number of corner-, edge-, and face-sharing bonds per one atom (Si or Mg), respectively.

P (GPa)	N_c	N_e	N_f
0	1.90	0.16	0.00
5	2.01	0.30	0.00
10	2.02	0.49	0.02
15	2.06	0.60	0.05
20	1.99	0.83	0.10
25	1.98	0.91	0.12
30	1.93	0.95	0.14
40	1.86	1.08	0.18
60	1.84	1.21	0.25
80	1.84	1.25	0.28
100	1.81	1.30	0.33

Table 5. The average bond length of corner-, edge- and face-sharing bond between Si–Mg at different pressure. Here, CSBL, ESBL and FSBL corresponding to corner-, edge- and face-sharing bond length.

P (GPa)	CSBL (Å)	ESBL (Å)	FSBL (Å)
0	3.26	2.79	—
5	3.26	2.81	2.65
10	3.27	2.83	2.67
15	3.28	2.83	2.65
20	3.31	2.86	2.66
25	3.32	2.85	2.64
30	3.33	2.84	2.64
40	3.34	2.83	2.62
60	3.36	2.81	2.58
80	3.35	2.78	2.56
100	3.35	2.76	2.55

the O–O distances that are calculated via equations (4a) and (4b) are about 2.20–2.30 Å and 2.40–2.50 Å corresponding to average O–O distance in SiO_x and MgO_n units. It can be seen that the value O–O distance in SiO_x (around 2.2–2.3 Å) is very near to the O–O distance in MgO_n (around 2.40–2.50 Å). That is why the two peaks of O–O PRDF merge into single peak at high pressure.

3.3. Glassy network structure

Investigation shows that the glassy network structure of Mg_2SiO_4 is split into SiO_x-clusters. The size distribution of clusters is strongly dependent on pressure. Table 6 shows the size distribution of SiO_x-clusters at different pressures.

It can be seen that at ambient pressure, the glassy-network structure consists of SiO_x-subets/clusters with size from several atoms to over two hundred atoms. The clusters with

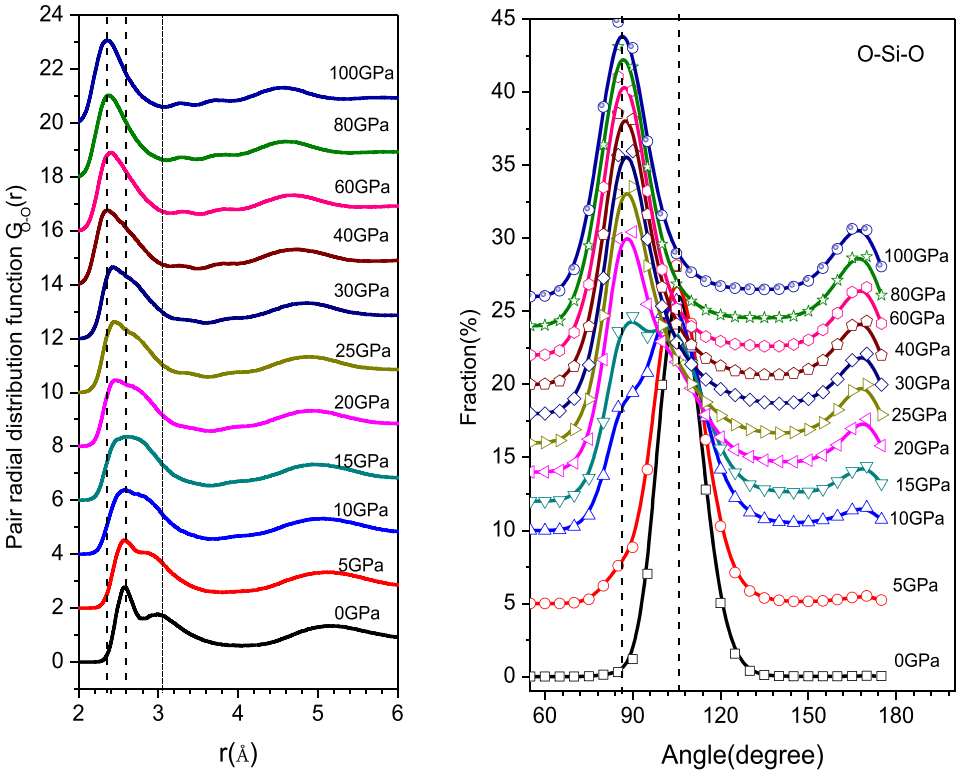

Figure 7. The O–O PRDF (left) and O–Si–O bond angle distribution (right) at different pressures (the vertical line is added into the plot to show the change of peak position under compression).

size of five atoms are the isolated SiO_4 units. Similarly, the clusters with size of six and seven atoms are the isolated SiO_5 and SiO_6 units. The largest SiO_x-cluster at ambient pressure consists of 249 atoms. Under compression, the small clusters tend to merge each other forming larger clusters. The number of isolated SiO_x ($x = 4, 5, 6$) units decreases strongly with pressure. At 10 GPa, the largest SiO_x-cluster consists of 2176 atoms. At pressure beyond 10 GPa, the size of largest cluster is over 3000 atoms. It means that most of SiO_x units in model link to each other. At pressure over 20 GPa, the glassy network of Mg_2SiO_4 consists of a large one with size of over 3000 atoms and several small ones with size of several atoms. The form of typical SiO_x-clusters is showed in figure 9. The above analysis demonstrates that the degree of polymerization of glassy network increases strongly with increasing pressure. To more clarify the degree of polymerization under compression, the distribution of Q^n units (Q is SiO_x units, n is the number of BOs belongs the SiO_x units). Figure 10 shows the distribution of Q^n as a function of pressure. It can be seen that at ambient pressure, most of SiO_x units only have one or two BOs, the number of SiO_x with three BOs is only about 10%. The number of SiO_x with more than three BOs is almost zero. Under compression, the number of Q^0, Q^1 and Q^2 units decreases strongly, meanwhile the number of Q^3, Q^4, Q^5 and Q^6 increases strongly. The number of Q^3 gets maximum value (about 26%–28%) at around 30 GPa. At pressure beyond 30 GPa, the number of Q^0, Q^1, Q^2 and Q^3 units decreases slightly

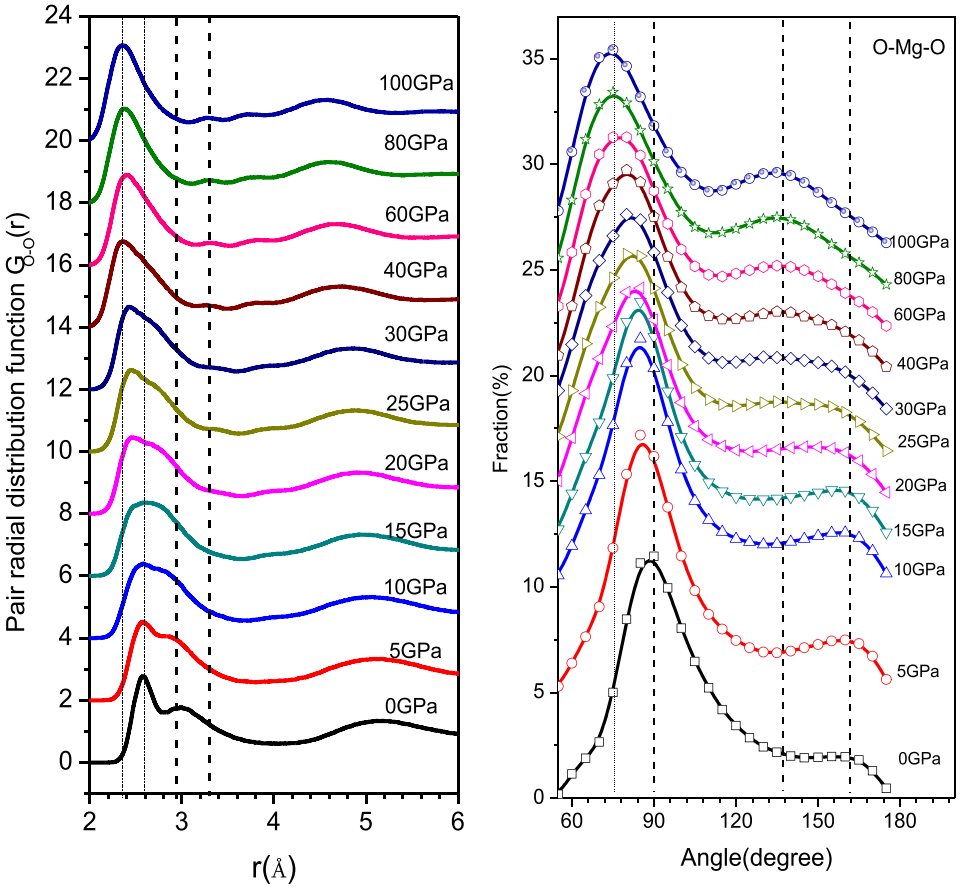

Figure 8. The O–O PRDF (left) and O–Mg–O bond angle distribution (right) at different pressures (the vertical line is added into the plot to show the change of peak position under compression).

with pressure, meanwhile the number of Q^4, Q^5 and Q^6 increases slightly with pressure. At 100 GPa, most of SiO_x units have three, four or five BOs. The number of Q^0 and Q^1 units at 100 GPa is very small. Meanwhile the number of Q^2 units is about 10%, similar to the number of Q^6 units. This result again demonstrates that the polymerization increases as pressure increases. The degree of polymerization of glassy network is dependent on the number of BOs. To more clarify this issue, the distribution of BOs, NBO and FO is calculated and showed in figure 11. It can be seen that the number of BOs is increases strongly with pressure in 0–40 GPa range. In contrast, the number of NBOs and FOs is decreases strongly with pressure. At ambient pressure, the fractions of BO, NBO and FO are about 18, 65 and 17%, respectively. At 40 GPa, the fractions of BO, NBO and FO are about 40, 50 and 10%, respectively. At pressure beyond 40 GPa, it changes slightly with pressure. At 100 GPa, the fractions of BOs, NBOs and FOs are about 46, 45 and 9%, respectively. This again demonstrates that the degree of polymerization increases strongly with pressure in the 0–40 GPa range and increases slightly at pressure beyond 40 GPa. The fraction of FOs is about 17% at ambient pressure. This demonstrates that it exists Mg-rich regions in the Mg_2SiO_4 glass. The analysis also shows that

Table 6. Size distribution of SiO_x-clusters at different pressure (0–100 GPa), where N_s is the number of subnets/clusters; N_a is the number of atoms per one cluster.

0 GPa		10 GPa		20 GPa		40 GPa		60 GPa		100 GPa	
N_s	N_a	N_s	N_a	N_s	N_a	N_s	N_a	N_s	N_a	N_s	N_a
144	5	78	5	18	5	6	5	1	5	1	6
37	9	4	6	6	6	6	6	5	6	2	7
23	13	8	9	2	7	2	7	1	11	1	3296
8	17	5	10	2	9	2	11	1	3250		
1	20	1	11	1	10	1	3168				
2	21	1	13	1	14						
1	22	4	14	1	17						
1	24	1	17	1	29						
6	25	2	18	1	3012						
2	28	1	19								
2	29	2	22								
1	30	1	27								
1	37	1	31								
1	38	1	49								
1	45	1	60								
1	56	1	62								
1	57	1	2176								
1	61										
2	69										
1	73										
1	75										
1	77										
1	81										
1	101										
1	114										
1	249										

it exists a lot of isolated SiO_x units. It means that, the Mg-rich regions is rather large that can contain one or several SiO_x units inside. This reveals the structural and compositional heterogeneity in Mg_2SiO_4 glass. Under compression, it forms edge- and face-sharing bonds between adjacent Si atoms. The interconnection between SiO_x relate to –Si–O– glassy network and IRO structure. To clarify the issue, the distribution of clusters of corner-, edge-, and face-sharing bonds and their size has been investigated and showed in tables 7–9. It can be seen that at ambient pressure, it only exists corner-sharing bonds between Si–Si in –Si–O- glassy network and this network is split into many subnets/clusters as shown in table 6 and figure 9. However, in tables 7–9, we focus on the type of bonds between Si–Si. It can be seen that at ambient pressure, the clusters of corner-sharing bonds have the size from three atoms (forming Si–O–Si cluster, an isolated bond) to 125 atoms, see table 7. There are 37 clusters with size of three atoms (Si–O–Si). It means that there are 37 clusters, each cluster consist of only two SiO_4 units (*two SiO_4 connects to each other forming a cluster with size of nine atoms. As shown in* table 6*, there are 37 clusters with size of nine atoms*). Figure 12 shows typical corner-sharing bond clusters at ambient pressure. It can be seen that the clusters have the form of chain- or tree-shape with one or several rings. Under compression, the small clus-

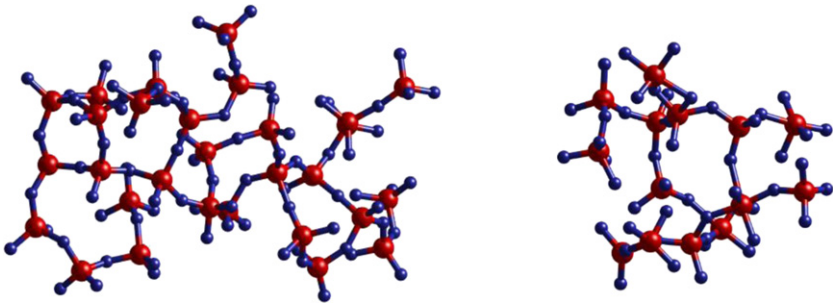

Figure 9. Typical SiO_x-clusters at ambient pressure: the clusters with size of 114 atoms (left) and 61 atoms (right).

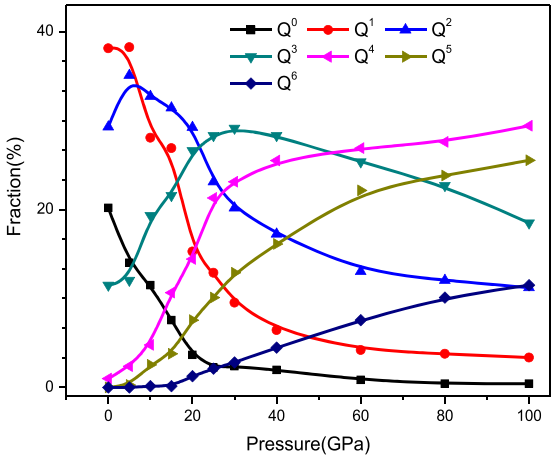

Figure 10. Distribution of Q^n units as a function of pressure.

ter of corner-sharing bonds tend to merge each other forming large one and the number of isolated bonds (Si–O–Si) decreases strongly with pressure. At pressure beyond 20 GPa, most of corner-sharing bonds connects to each other forming a large one and only remain several small ones with size from three to nine atoms, see table 7. The edge- and face-sharing bonds begin to form at pressure beyond 10 GPa. The edge- and face-sharing bonds are not uniformly distributed in model, but they tend forming clusters. The size of clusters increases strongly with pressure. At 100 GPa, the largest cluster of edge-sharing bonds has the size of 79 atoms. While, the largest cluster of face-sharing bonds has the size of 15 atoms, see tables 8 and 9. The typical clusters of edge-, and face-sharing bonds are showed in figures 13 and 14 respectively. The above analysis reveals that the –Si–O– glassy network comprises three types of bonds forming three types of subnets/clusters. It means that –Si–O– glassy network is the mixture of three subnets/clusters: cluster of corner-sharing bonds, see figure 12; cluster of edge-sharing bonds, see figure 13; cluster of face-sharing bonds, see figure 14. The face-sharing bond is very stable. With small size and very stable, the clusters of face-sharing bonds can be consid-

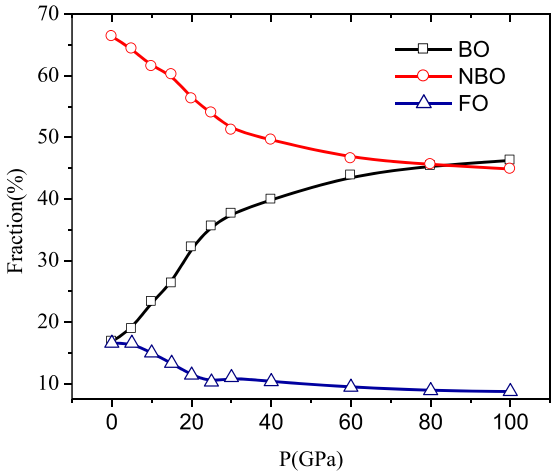

Figure 11. Distribution of BO, NBO and FO as a function of pressure.

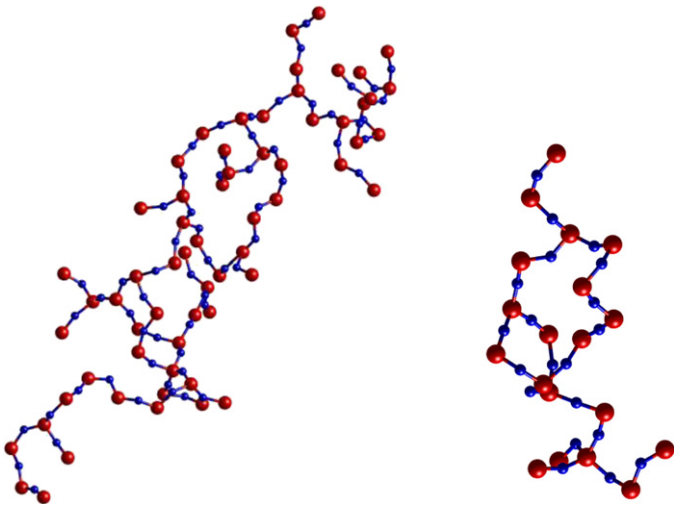

Figure 12. Typical corner-sharing bond clusters at ambient pressure: clusters with size of 125 atoms (left) and 39 atoms (right).

ered as rigid-clusters (the same as 'hard particles'). Therefore, it can be considered that the –Si–O– glassy network of Mg_2SiO_4 consists of rigid-clusters embedding in the mixture network of corner- and edge-sharing bonds. This one again shows the structural heterogeneity in Mg_2SiO_4 glass, see figure 15.

3.4. Mechanism of Mg ion incorporation into –Si–O– glassy network

To clarify the mechanism of Mg ion incorporation into –Si–O– glassy network, the distribution of OT_y linkages (T = Si, Mg; y = 2–7) has been calculated and shown in figures 16

Table 7. Size distribution of corner-sharing Si–Si bond subnets/clusters at different pressures, where N_s is the number of subnets/clusters; N_a is the number of atoms per one cluster.

0 GPa		10 GPa		20 GPa		40 GPa		60 GPa		100 GPa	
N_s	N_a	N_s	N_a	N_s	N_a	N_s	N_a	N_s	N_a	N_s	N_a
37	3	16	3	6	3	2	3	1	3	1	3
23	5	3	5	4	5	1	1575	1	5	1	9
8	7	5	7	1	7			1	1581	1	1611
3	9	1	9	1	1431						
1	10	1	12								
6	11	1	13								
1	12	2	17								
3	13	1	19								
2	14	2	25								
2	17	1	26								
1	21	2	30								
1	27	1	35								
1	28	1	910								
1	29										
2	33										
1	35										
1	37										
2	39										
1	49										
1	60										
1	125										

and 17. It can be seen that the OT_2 linkages only exist at low pressure ($p < 15$ GPa) and have small fraction. Meanwhile, the OT_7 linkages only exist at high pressure and have very small fraction. Most of OT_2 linkages are O(2Si), it means that one O^{2-} ion links to 2 Si^{4+} ions forming Si–O–Si linkage. In this case, the O atom is BO. The number of O(2Si) is about 8.5% at ambient pressure and it decreases strongly with pressure. The fraction of O(2Si) is almost zero at pressure beyond 40 GPa. The number of O(Si, Mg) forming Si–O–Mg linkages is about 2.5% at ambient pressure and it decreases strongly with pressure. The number of Si–O–Mg linkages is almost zero at pressure beyond 10 GPa. The number of OT_7 linkages is very small and they only exist two types: O(7Mg) and O(Si, 6Mg). The largest fractions of O(7Mg) and O(Si, 6Mg) are about 0.010 and 0.015%, respectively, (at 100 GPa). For OT_3 linkages, most of them are O(Si, 2Mg) and O(2Si, Mg). The fraction of O(Si, 2Mg) decrease strongly from 38% at ambient pressure to zero at 40 GPa. The fraction of O(2Si, Mg) increase from about 8% at ambient pressure to maximum value of approximately 12% at 10 GPa then decrease gradually to about 2% at 100 GPa. The other OT_3 linkages O(3Mg), O(3Si) is very small, see figure 17. For OT_4 linkages, it can be seen that most of them are O(Si, 3Mg), O(4Mg) and O(2Si, 2Mg). The fraction of O(Si, 3Mg) increases from about 25% (at ambient pressure) to the maximum value of approximately 35% (at 10 GPa) then it decreases strongly to about 8% at (100 GPa). The fraction of O(4Mg) decrease from 11% (at ambient pressure) to zero (at pressure beyond 40 GPa). The fraction of O(2Si, 2Mg) increases from zero (at ambient pressure) to approximately 18% (at 25 GPa), then decreases slightly

Table 8. Size distribution of edge-sharing Si–Si bond subnets/clusters at different pressures, where N_s is the number of subnets/clusters; N_a is the number of atoms per one cluster.

0 GPa		10 GPa		20 GPa		40 GPa		60 GPa		100 GPa	
N_s	N_a	N_s	N_a	N_s	N_a	N_s	N_a	N_s	N_a	N_s	N_a
—	—	20	4	59	4	63	4	58	4	47	4
—	—	—	—	2	6	7	6	6	6	11	6
—	—	—	—	6	7	11	7	14	7	8	7
—	—	—	—	1	8	2	8	3	8	3	8
—	—	—	—	1	14	4	9	3	9	4	9
—	—	—	—	—	—	4	10	5	10	5	10
—	—	—	—	—	—	4	11	3	11	1	11
—	—	—	—	—	—	1	12	4	12	1	12
—	—	—	—	—	—	1	15	1	13	2	14
—	—	—	—	—	—	1	18	1	14	1	15
—	—	—	—	—	—			2	15	1	16
—	—	—	—	—	—	—	—	1	17	2	18
—	—	—	—	—	—	—	—	1	20	1	19
—	—	—	—	—	—	—	—	1	21	2	20
—	—	—	—	—	—	—	—	2	22	1	23
—	—	—	—	—	—	—	—	1	27	1	26
—	—	—	—	—	—	—	—	1	38	1	28
—	—	—	—	—	—	—	—	1	52	1	38
—	—	—	—	—	—	—	—	—	—	1	42
—	—	—	—	—	—	—	—	—	—	1	72
—	—	—	—	—	—	—	—	—	—	1	79

Table 9. Size distribution of face-sharing Si–Si bond subnets/clusters at different pressures, where N_s is the number of subnets/clusters; N_a is the number of atoms per one cluster.

0 GPa		10 GPa		20 GPa		40 GPa		60 GPa		100 GPa	
N_s	N_a	N_s	N_a	N_s	N_a	N_s	N_a	N_s	N_a	N_s	N_a
—	—	2	5	4	5	15	5	15	5	21	5
—	—	—	—	—	—	—	—	1	7	1	10
—	—	—	—	—	—	—	—	—	—	1	15

to approximately 16% (at 100 GPa). The fraction of other OT_4 linkage types is very small. The fraction of O(3Si, Mg) increases from zero (at ambient pressure) to about 3% (at 40 GPa). At pressure beyond 40 GPa, it is almost unchanged. For OT_5 linkages, most of them are O(5Mg), O(Si, 4Mg), O(3Si, 2 Mg) and O(3Si, 2 Mg). The fraction of O(5Mg) increases from zero (at ambient pressure) to 5% (at 10 GPa) then it decreases gradually to about 3% (at 100 GPa). The fraction of O(Si, 4Mg) increases abruptly from about 1% (at ambient pressure) to approximately 24% (at 25 GPa) then decreases slightly to 23% (at 100 GPa). The fraction of O(2Si, 3Mg) increases from zero (at ambient pressure) to 18% (at 100 GPa). The fraction of O(3Si, 2Mg) increases from zero (at ambient pressure) to approximately 2.5% (at

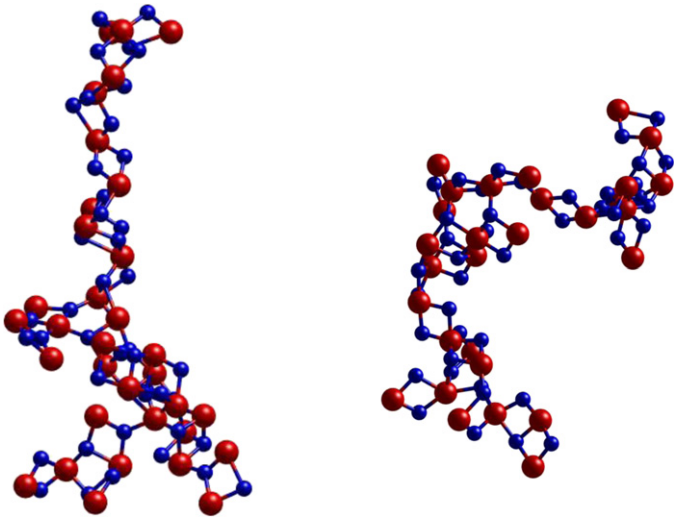

Figure 13. Typical edge-sharing clusters at 100 GPa: clusters with size of 79 atoms (left) and 72 atoms (right). The small sphere is O atom; the large sphere is Si atom.

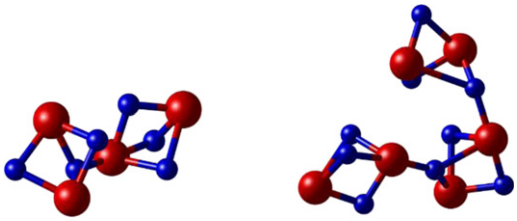

Figure 14. Typical face-sharing bond clusters at 100 GPa: clusters with size of 10 atoms (left) and 15 atoms (right).

100 GPa). For OT_6 linkages, it only exists three types: O(6Mg), O(Si, 5Mg) and O(2Si, 4Mg). These linkages tend to increase with pressure from zero (at ambient pressure) to 5, 13, 5% for O(6Mg), O(Si, 5Mg) and O(2Si, 4Mg), respectively (at 100 GPa).

The above analysis reveals that, the Mg^{2+} ions tend to link with –Si–O– glassy network via NBO. At low pressure, each NBO tends to link to one, two or three Mg^{2+} ions. At high pressure, each NBO can link to four, five or six Mg^{2+} ions. At low pressure, it also exists a significant fraction of FO, and the Mg^{2+} ions also tend to link to FOs forming the Mg-rich regions. As pressure increases, the fraction of NBO and FO decreases, see figure 11. Therefore, at high pressure, the Mg^{2+} ions tend to link to –Si–O– glassy network via both NBOs and BOs. At low pressure, the Mg^{2+} ions tend to link to SiO_x in –Si–O– glassy network via one common O^{2-} ion forming corner-sharing bonds between Si^{4+} ions and Mg^{2+} ones). Under compression, it forms the edge-sharing bonds and face-sharing between Si^{4+} ions and Mg^{2+} ones, see table 4. The distribution of edge-sharing and face-sharing bonds between Si^{4+} and Mg^{2+} ions in model is not uniform but they tend to form cluster, see table 10. The typical clusters of edge-sharing bonds are shows in figure 18. The clusters of face-sharing bonds are shown in figure 19.

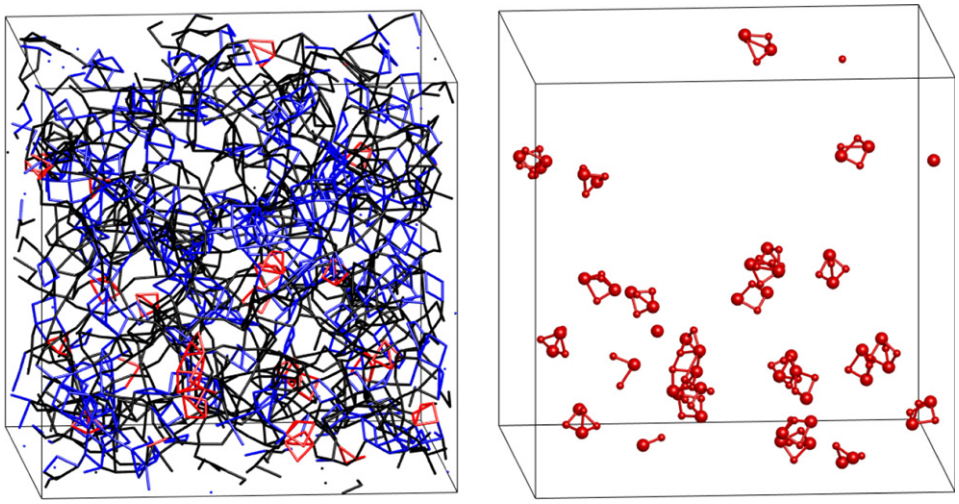

Figure 15. Spatial distribution of clusters in model: corner-sharing Si–Si bonds in black; edge-sharing Si–Si bonds in blue; face-sharing Si–Si bonds in red. Mixture of corner-, edge- and face-sharing bonds (left) and cluster of face-sharing bonds (right).

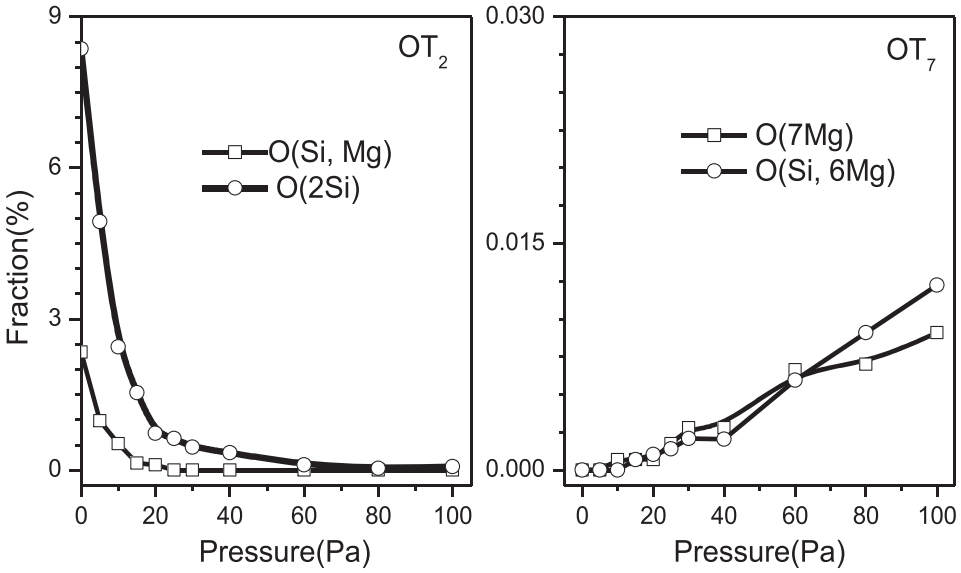

Figure 16. Fraction distribution of oxygen atoms forming OT_2 and OT_7 linkages in Mg_2SiO_4 glass as a function of pressure.

4. Discussion

The local structure and network structure of Mg_2SiO_4 under compression (0–100 GPa) have investigated in detail. The change of structural characteristics (SRO and IRO) and network

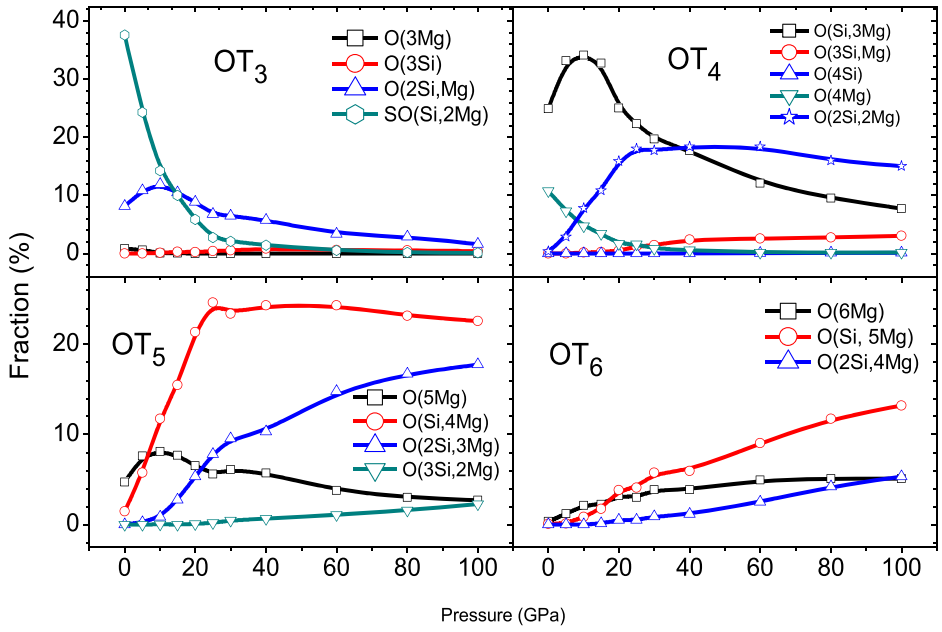

Figure 17. Fraction distribution of oxygen atoms forming OT_x ($x = 3, 4, 5, 6$) linkages in Mg_2SiO_4 glass as a function of pressure.

structure as well as the mechanism of Mg ion incorporation into –Si–O– glassy network have been clarified.

Relate to local structure and topology of SiO_x units, the results show that the Si–O bond length in SiO_6 > the one in SiO_5 > the one SiO_4 units, see figure 3. In addition, the number of SiO_5 and SiO_6 units increases strongly with pressure in 0–40 GPa range, see figure 2. Therefore, Si–O bond length in Mg_2SiO_4 tends to increase with pressure. That is why the first peak position of Si–O PRDF tends to shift to right with pressure in 0–40 GPa range. At pressure beyond 40 GPa, the compression makes the Si–O bond length in SiO_x decreases strongly (see figure 3) meanwhile the increase of Si–O bond length due to the increases of coordination is small (see figure 2). That is why the first peak position of Si–O PRDF tends to shift to left with pressure in 40–100 GPa range. The O–Si–O BAD in SiO_5 and SiO_6 units almost does not change with pressure meanwhile the Si–O bond length in SiO_5 and SiO_6 units decreases with pressure, see figure 3. This reveals that the form of SiO_5 and SiO_6 units is almost not dependent on pressure, but their size decreases significantly under compression. In contrast, the topology of SiO_4 units is strongly distorted under compression (both form and size change with pressure).

For Intermediate range order, the results show that the SiO_x ($x = 4, 5, 6$) units can link to each other via one, two or three BOs forming corner-, edge- or face-sharing bonds, respectively. At low pressure ($P < 15$ GPa), most of SiO_x units are SiO_4 tetrahedra linking to each other via corner-sharing bonds and the average Si–Si distance is around 3.10 Å. Under compression, the SiO_4 tetrahedra tend to transform to SiO_6 octahedra via SiO_5 units. At high pressure ($P > 20$ GPa), most of SiO_x are SiO_5 and SiO_6 and they can link to each other via corner-, edge- or face-sharing bonds. However, the number of face-sharing bonds is very small in comparison to the other types. The average Si–Si distance of corner-, edge- and face-sharing bonds are around 3.10, 2.80 and 2.55 Å, respectively. The existence of the corner-, edge- and

Table 10. Size distribution of corner-, edge and face-sharing Mg–Si bond subnet/clusters at different pressures, where N_s is the number of subnets/clusters; N_a is the number of atoms per one subnet/cluster.

0 GPa		10 GPa		20 GPa		40 GPa		60 GPa		100 GPa	
N_s	N_a	N_s	N_a	N_s	N_a	N_s	N_a	N_s	N_a	N_s	N_a
Size distribution of corner-sharing bond clusters											
1	4234	1	4357	1	4434	1	4360	1	4363	1	4355
Size distribution of edge-sharing bond subnets/clusters											
65	4	1	4	1	3851	1	4195	1	4291	1	4343
24	5–10	1	6								
16	11–20	1	2961								
8	21–40										
5	41–60										
1	68										
1	114										
1	184										
Size distribution of face-sharing bond subnets/clusters											
1	5	26	5	33	5	10	5	1	5	1	2638
		3	7	16	6–20	1	7	1	2194		
		2	8	1	24	1	14				
		1	9	1	27	1	21				
		4	10	1	31	1	27				
		2	16	1	53	1	29				
		1	18	1	64	1	1577				
		1	20	1	106						
				1	133						
				1	223						

face-sharing bonds with different bond length is the origin of the first peak splitting of Si–Si PRDF [44].

The Mg ions tend incorporate into –Si–O– glassy network via NBOs (at low pressure) and via both NBOs and BOs (at high pressure). The results also show that the Mg ions can link to SiO_x via one, two or three O atoms forming corner-, edge- and face-sharing bonds, respectively. The average Mg–Si distance of corner-, edge- and face-sharing bonds are around 3.30, 2.80 and 2.60 Å, respectively. This explains why the PRDF of Si–Mg pair having the peak at around 2.6–2.80 Å and a peak or shoulder (peak at low pressure, shoulder at high pressure) at around 3.30 Å.

The structure of Mg_2SiO_4 comprises SiO_x and MgO_n units. At ambient pressure the average Si–O and Mg–O coordination number are around 4.0 and 4.75, respectively, see figure 2. The O–O distance in SiO_x units is dependent on O–Si–O bond angle. Similarly, the O–O distance in MgO_n is dependent on the O–Mg–O bond angle. In other word, the O–O distance in SiO_x and MgO_n units depends on the Si–O and Mg–O coordination number. Under compression, the Si–O and Mg–O coordination number increases accompanying the decrease of O–Si–O and O–Mg–O bond angle. This results in the decrease of O–O distance. At low

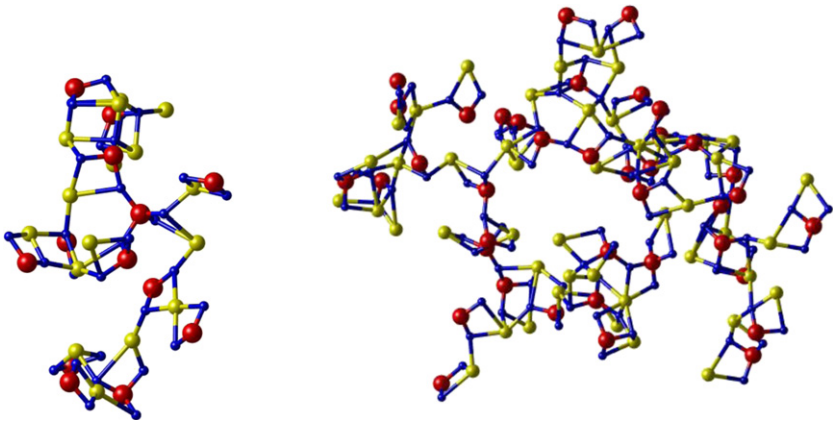

Figure 18. Typical clusters of edge-sharing bond between Si and Mg. The cluster of 60 atoms (left) and 184 atoms (right). The spheres from small to large are O, Mg and Si, respectively.

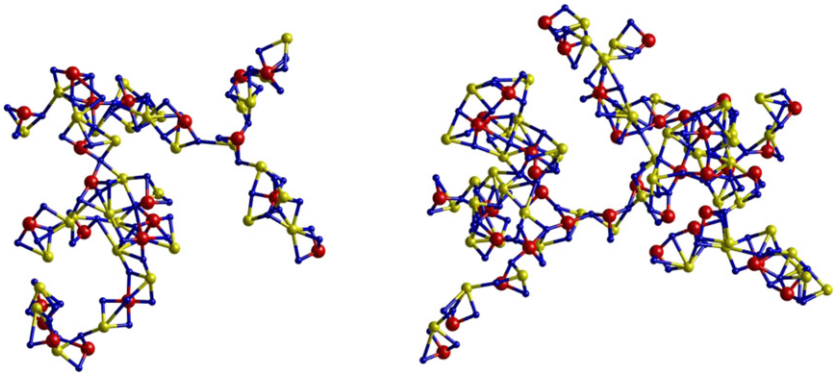

Figure 19. Typical cluster of face-sharing bonds between Si and Mg. The cluster of 133 atoms (left) and 223 atoms (right), the spheres from small to large are O, Mg and Si, respectively.

pressure, the O–O distance in SiO_x and MgO_n is significantly different (around 2.40–2.60 Å and 2.90–3.00 Å corresponding to O–O distance in SiO_x and MgO_n). This is the origin of first peak splitting of O–O PRDF at low pressure, see figure 8.

The results also reveal a tight correlation between PRDFs and BAD at different pressures. The Si–Si, Mg–Mg, Mg–Si, O–O distance can be determined by using the equations (1), (2), (3) and (4a), (4b), respectively. Under compression, the structure (SRO and IRO) of Mg_2SiO_4 changes that results in the change of Si–O–Si, Mg–O–Mg, Mg–O–Si, O–Si–O and O–Mg–O bond angle. This leads to the change of Si–Si, Mg–Mg, Mg–Si, O–O distance. It means that the characteristic change of PRDFs under compression in the relationship with microstructural change can be clarified via equations (1)–(4b).

Relate to network structure, it can be seen that at ambient pressure, the –Si–O– glassy network in Mg_2SiO_4 glass is split into subnets. Under compression, the polymerized degree of –Si–O– glassy network increases strongly and subnets tend to merge each other forming

larger ones, see table 6. At low pressure, the SiO_x units in –Si–O– glassy network tend to link to each other via corner-sharing bonds. Under compression, the number of BOs in –Si–O– glassy network increases and it forms edge- and face- sharing bonds between SiO_x units. The spatial distribution of corner-, edge- and face- sharing bonds is not uniform. This reveals the structural heterogeneity of –Si–O– glassy network in Mg_2SiO_4 glass under compression, see figure 15.

For mechanism of Mg ion incorporation into –Si–O– glassy network, the results reveal that the Mg^{2+} ions tend to link with –Si–O– glassy network via NBOs. At low pressure, each NBO tends to link to one, two or three Mg^{2+} ions. At high pressure, each NBO can link to four, five or six Mg^{2+} ions. At low pressure, it also exists a significant fraction of FO, and the Mg^{2+} ions also tend to link to FOs forming the Mg-rich regions. As pressure increases, the fraction of NBO and FO decreases, see figure 11. Therefore, at high pressure, the Mg^{2+} ions tend to link to –Si–O– glassy network via both NBOs and BOs. At low pressure, the Mg^{2+} ions tend to link to SiO_x in –Si–O– glassy network via one common O^{2-} ion forming corner-sharing bonds between Si^{4+} ions and Mg^{2+} ones). Under compression, it forms the edge-sharing and face-sharing bonds between Si^{4+} ions and Mg^{2+} ones, see table 4. The distribution of edge-sharing and face-sharing bonds between Si^{4+} and Mg^{2+} ions in model is not uniform but they tend to form clusters, see table 10. The typical clusters of edge-sharing bonds are shows in figure 18. The clusters of face-sharing bonds are shown in figure 19.

5. Conclusion

The form of SiO_5 and SiO_6 polyhedra is almost not changed under compression. However, the SiO_4 tetrahedra is distorted as pressure increases.

At ambient pressure, the –Si–O– glassy network in Mg_2SiO_4 glass is split into subnets/clusters. Under compression, the subnets/clusters tend to merge each other forming larger subnets/clusters. The degree of polymerization of –Si–O– network increases with pressure.

There is a tight correlation between the PRDFs and corresponding BADs, BLDs. The Si–Si, Mg–Mg, Si–Mg and O–O distances can be determined via corresponding BADs and T–O BLDs. The formation of edge- and face sharing bonds between SiO_x units at high pressure is the cause of the first peak splitting of Si–Si PRDF. The correlation between the microstructural characteristics (BAD, BLD) and the peaks of PRDFs support us a method to determine the microstructural change of Mg_2SiO_4 glass under compression.

The number of corner-, edge- and face sharing Si–Si bonds increases as pressure increases. They are not uniformly distributed in model but forming clusters. The clusters of face-sharing Si–Si bond clusters are small and very stable. These face-sharing Si–Si bond clusters are considered as rigid-particles (or hard particle). The –Si–O– glassy network comprises the rigid-particles of face-sharing Si–Si bonds embedding in mixture network of corner- and edge-sharing Si–Si bonds.

The Mg^{2+} ions tend to link to –Si–O– glassy network via NBOs (at low pressure) and via both NBOs and BOs (at high pressure). Mg^{2+} ions can incorporate in –Si–O– glassy network via corner-, edge- and face sharing Mg–Si bonds. These bond types are not uniformly distributed but forming clusters. It also exists the Mg-rich regions in model of Mg_2SiO_4 glass. This demonstrates the structural and compositional heterogeneities in magnesium silicate glass.

Acknowledgments

This research is funded by Vietnam National Foundation for Science and Technology Development (NAFOSTED) under grant number: 103.05-2018.38

Conflict of interest

The authors declare that they have no conflict of interest.

Appendix A.

See table A1.

Table A1. List of abbreviations.

Abbreviations	Definition	Abbreviations	Definition
PRDF	Pair radial distribution function	CSBL	Corner-sharing bond length
BAD	Bond angle distribution	MD	Molecular Dynamics
SRO	Short range order	BLD	Bond length distribution
IRO	Intermediate range order	ESBL	Edge-sharing bond length
NMR	Nuclear magnetic resonance	FSBL	Face-sharing bond length
RMC	Reverse Monte Carlo	N_c	The average number of corner -sharing bonds per one atom
BO	Bridge oxygen	N_e	The average number of edge -sharing bonds per one atom
NBO	Non-bridge oxygen	N_f	The average number of face -sharing bonds per one atom
FO	Free oxygen	N_s	The number of subnets/cluster
		N_a	The number of atoms per one subnet/cluster

ORCID iDs

Nguyen Van Hong https://orcid.org/0000-0002-0097-9840

References

[1] Karki B B and Stixrude L P 2010 Viscosity of $MgSiO_3$ liquid at Earth's mantle conditions: implications for an early magma ocean *Science* **328** 740–42
[2] Sakai T *et al* 2016 Experimental and theoretical thermal equations of state of $MgSiO_3$ post-perovskite at multi-megabar pressures *Sci. Rep.* **6** 22652
[3] Tomioka N and Okuchi T 2017 A new high-pressure form of Mg_2SiO_4 highlighting diffusionless phase transitions of olivine *Sci. Rep.* **7** 17351
[4] Gavin M, Al-Hasni B M and Storey C 2011 Structural organisation in oxide glasses from molecular dynamics modelling *J. Non-Cryst. Solids* **357** 2522–29
[5] Pedone A, Malavasi G, Cristina Menziani M, Segre U and Cormack A N 2008 Role of magnesium in soda-lime glasses: insight into structural, transport, and mechanical properties through computer simulations *J. Phys. Chem* C **112** 11034–41
[6] Lina C-C, Chenb S-F, Liua L and Lia C 2007 Anionic structure and elasticity of Na_2O–MgO–SiO_2 glasses *J. Non-Cryst. Solids* **353** 413–25
[7] Cormier L and Cuello G J 2011 Mg coordination in a $MgSiO_3$ glass using neutron diffraction coupled with isotopic substitution *Phys. Rev.* B **83** 224204

[8] Wilding M C, Benmore C J, Tangeman J A and Sampath S 2004 Coordination changes in magnesium silicate glasses *Europhys. Lett.* **67** 212–8
[9] Taniguchi T, Okuno M and Matsumoto T 1997 X-ray diffraction and EXAFS studies of silicate glasses containing Mg, Ca and Ba atoms *J. Non-Cryst. Solids* **211** 56
[10] Shimoda K, Tobu Y, Hatakeyama M, Nemoto T and Saito K 2007 Structural investigation of Mg local environments in silicate glasses by ultra-high field 25Mg 3QMAS NMR spectroscopy *Am. Mineral.* **92** 695–8
[11] Sen S, Maekawa H and Papatheodorou G N 2009 Short-range structure of invert glasses along the pseudo-binary join $MgSiO_3$–Mg_2SiO_4: results from 25Si and 25Mg MAS NMR Spectroscopy *J. Phys. Chem* B **113** 15243–8
[12] Kohara S, Akola J, Morita H, Suzuya K, Weber J K R, Wilding M C and Benmore C J 2011 Relationship between topological order and glass forming ability in densely packed enstatite and forsterite composition glasses *PNAS* **108** 14780–5
[13] Benmore C J, Soignard E, Guthrie M, Amin S A, Weber J K R, McKiernan K, Wilding M C and Yarger J L 2011 High pressure x-ray diffraction measurements on Mg_2SiO_4 glass *J. Non-Cryst. Solids* **357** 2632
[14] Wilding M C Benmore C J, Tangemanc J A and Sampath S 2004 Evidence of different structures in magnesium silicate liquids: coordination changes in forsterite- to enstatite-composition glasses *Chem. Geol.* **213** 281–91
[15] Guignard M and Cormier L 2008 Environments of Mg and Al in MgO–Al_2O_3–SiO_2 glasses: a study coupling neutron and x-ray diffraction and Reverse Monte Carlo modeling *Chem. Geol.* **256** 111–8
[16] Wilding M C, Benmore C J and Weber J K R 2008 *In situ* diffraction studies of magnesium silicate liquids *J. Mater. Sci.* **43** 4707–13
[17] Zhang P and Grandinetti P J 1997 Anionic species determination in $CaSiO_3$ glass using two-dimensional 29Si NMR *J. Phys. Chem.* B **101** 4004–8
[18] Lee S K *et al* 2008 X-ray Raman scattering study of $MgSiO_3$ glass at high pressure: implication for triclustered $MgSiO_3$ melt in Earth's mantle *Proc. Natl Acad. Sci.* **105** 7925–9
[19] Matsui Y and Kawamura K 1980 Instantaneous structure of an $MgSiO_3$ melt simulated by molecular dynamics *Nature* **285** 648–9
[20] Kubicki J D and Lasaga A C 1991 Molecular dynamics simulations of pressure and temperature effects on $MgSiO_3$ and Mg_2SiO_4 melts and glasses *Phys. Chem. Miner.* **17** 661–73
[21] Spera F J, Ghiorso M S and Dean N 2011 Structure, thermodynamic and transport properties of liquid $MgSiO_3$: Comparison of molecular models and laboratory results *Geochim. Cosmochim. Acta* **75** 1272–96
[22] Ben Martin G, Spera F J, GhiorSo M S and Nevins N 2009 Structure, thermodynamic and transport properties of liquid $MgSiO_3$: comparison of molecular models and laboratory results *Am. Mineral.* **94** 693
[23] Chaplot S L and Choudhury N 2001 Molecular dynamics simulations of seismic discontinuities and phase transitions of $MgSiO_3$ from 4 to 6-coordinated silicate via a novel 5-coordinated phase *Am. Mineral.* **86** 752–61
[24] de Koker N P, Stixrude L and Karki B B 2008 Thermodynamics, structure, dynamics, and freezing of Mg_2SiO_4 liquid at high pressure *Geochim. Cosmochim. Acta* **72** 1427–41
[25] Omar A, Steinle-Neumann G and Jahn S 2008 Mg_2SiO_4 liquid under high pressure from molecular dynamics *Chem. Geol.* **256** 185–92
[26] Zhao G, Mu H F, Tan X M, Wang D H and Yang C L 2014 Structural and dynamical properties of $MgSiO_3$ melt over the pressure range 200–500 GPa: *ab initio* molecular dynamics *J. Non-Cryst. Solids* **385** 169–74
[27] Ghosh D B, Karki B B and Stixrude L 2014 First-principles molecular dynamics simulations of $MgSiO_3$ glass: structure, density, and elasticity at high pressure *Am. Mineral.* **99** 1304–14
[28] Lacks D J, Rear D B and Van Orman J A 2007 Molecular dynamics investigation of viscosity, chemical diffusivities and partial molar volumes of liquids along the MgO-SiO_2 join as functions of pressure *Geochim. Cosmochim. Acta* **71** 1312–23
[29] Dean N, Spera F J and Ghiorso M S 2009 Shear viscosity and diffusion in liquid $MgSiO_3$: transport properties and implications for terrestrial planet magma oceans *Am. Mineral.* **94** 975–80

[30] Oganov A R, Brodholt J P and David Price G 2000 Comparative study of quasiharmonic lattice dynamics, molecular dynamics and Debye model applied to $MgSiO_3$ perovskite *Phys. Earth Planet. Int.* **122** 277–88
[31] Liu Z-J, Zhang C-R, Sun X-W, Hu J-B, Song T and Chu Y-D 2011 The melting curve of $MgSiO_3$ perovskite from molecular dynamics simulation *Phys. Scr.* **83** 045602
[32] Goryaeva A M, Carrez P and Cordier P 2015 Modeling defects and plasticity in $MgSiO_3$ post-perovskite: part 2—screw and edge [100] dislocations *Phys. Chem. Miner.* **42** 793
[33] Liu Z-J, Sun X-W, Tan X-M, Guo Y-D and Yang X-D 2007 Structural and thermodynamic properties of $MgSiO_3$ perovskite under high pressure and high temperature *Solid State Commun.* **144** 264–8
[34] Gaudio S J, Sen S and Lesher C E 2008 Pressure-induced structural changes and densification of vitreous $MgSiO_3$ *Geochim. Cosmochim. Acta* **72** 1222–30
[35] San L T, Van Hong N, Iitaka T and Pham K H 2016 Structural organization, micro-phase separation and polyamorphism of liquid $MgSiO_3$ under compression *Eur. Phys. J.* B **89** 73
[36] Guillot B and Sator N 2007 A computer simulation study of natural silicate melts. Part I: low pressure properties *Geochim. Cosmochim. Acta* **71** 1249–65
[37] Guillot B and Sator N 2007b A computer simulation study of natural silicate melts. Part II: high pressure properties *Geochim. Cosmochim. Acta* **71** 4538–56
[38] Kohara S, Suzuya K, Takeuchi K, Loong C K, Grimsditch M, Weber J K R, Tangeman J A and Key T S 2004 Glass formation at the limit of insufficient network formers *Science* **303** 1649–52
[39] Al-Hasni B M and Gavin M 2014 A molecular dynamics study of the atomic structure of x(MgO)100 $-$ $x(SiO_2)$ *J. Non-Cryst. Solids* **389** 33–4
[40] Salmon P S *et al* 2019 Pressure induced structural transformations in amorphous $MgSiO_3$ and $CaSiO_3$ *J. Non-Cryst. Solids* **3** 100024
[41] Martínez-González J Á, Navarro-Ruiz J and Albert R 2018 Multiscale computational simulation of amorphous silicates' structural, dielectric, and vibrational spectroscopic properties *Minerals* **8** 353
[42] Bidault X, Chaussedent S and Blanc W 2015 A simple transferable adaptive potential to study phase separation in large-scale xMgO–$(1 - x)SiO_2$ binary glasses *J. Chem. Phys.* **143** 154501
[43] Shimoda K and Okuno M 2006 Molecular dynamics study of $CaSiO_3$–$MgSiO_3$ glasses under high pressure *J. Phys.: Condens. Matter.* **18** 6531–44
[44] Nhan N T, Trang G T T, Iitaka T and Van Hong N 2019 Crystallization of amorphous silica under compression *Can. J. Phys.* **97** 1133–9